J|A|C|S COMMUNICATIONS

Published on Web 05/10/2010

Rationally Simplified Bistramide Analog Reversibly Targets Actin Polymerization and Inhibits Cancer Progression *in Vitro* and *in Vivo*

Syed Alipayam Rizvi,[†] Song Liu,[†] Zhonglei Chen,[†] Colleen Skau,[‡] Matthew Pytynia,[§] David R. Kovar,[‡] Steven J. Chmura,[§] and Sergey A. Kozmin*,[†]

University of Chicago, Department of Chemistry, Department of Molecular Genetics and Cell Biology, Department of Cellular and Radiation Oncology, Chicago, Illinois 60637

Received March 3, 2010; E-mail: skozmin@uchicago.edu

Cytoskeletal organization is strongly altered upon malignant transformation and tumor invasion, which includes significant changes in expression of actin and actin-binding proteins.[1] Small molecules that target the actin cytoskeleton could be potentially employed to study such alterations *in vivo* and ultimately combat cancer.[2] Bistramides comprise a polyketide-based family of natural products with potent antiproliferative activities, which was isolated from tunicates *L. bistratum* and *T. cyclops*.[3−6] Chemical synthesis of bistramide A (**1**, Figure 1)[7,8] enabled subsequent determination of the mechanism of action, which entailed specific modulation of the actin cytoskeleton[9,10] and covalent modification of the protein target.[11] Importantly, the actin-severing activity of this agent was not dependent on the covalent protein modification.[11] This observation suggested that rationally designed compounds, which do not react covalently with actin, may be able to target the actin cytoskeletion of cancer cells *in vivo*. Indeed, bistramides D and K that lack the reactive enone subunit were shown to inhibit proliferation of nonsmall cell broncho-pulmonary carcinoma implanted in nude mice.[12] In this communication, we describe structure-based design and synthesis of a simplified analog of bistramide A, which reversibly binds monomeric actin, efficiently depolymerizes filamentous actin, inhibits growth of cancer cell lines *in vitro*, and suppresses A549 (nonsmall cell lung cancer) tumor growth *in vivo*.

The structure of bistramide A can be dissected into three main fragments, including C(19)−C(38) spiroketal-bearing subunit **A**, C(13)−C(18) bisamide subunit **B**, and C(1)−C(13) enone-containing subunit **C** (Figure 1). Subunits **A** and **B** are required for binding of the natural product to its target by forming extended networks of hydrogen-bonding and van der Waals interactions, respectively.[10] The 1,3-enone moiety present in subunit **C** is responsible for covalent interaction of bistramide A with G-actin but not required for actin-severing activity.[11] Thus, removal of the highly reactivity enone-containing subunit **C** was expected to provide access to a simplified congener **2** (Figure 1) that could reversibly interact with the actin cytoskeleton and inhibit tumor growth *in vitro* and *in vivo*. The main challenge, however, was to preserve the potent bioactivity of this chemical agent while significantly simplifying the structure of the parent natural product. Indeed, while we previously demonstrated that structural simplifications of the bistramide framework were possible, such modifications typically decreased actin-binding and actin-severing activity of the resulting analogs, in some cases substantially.[11] Retention of the fully elaborated spiroketal subunit **A**, as well as the intact central amide fragment **B**, was expected to preserve the majority of hydrophobic and polar

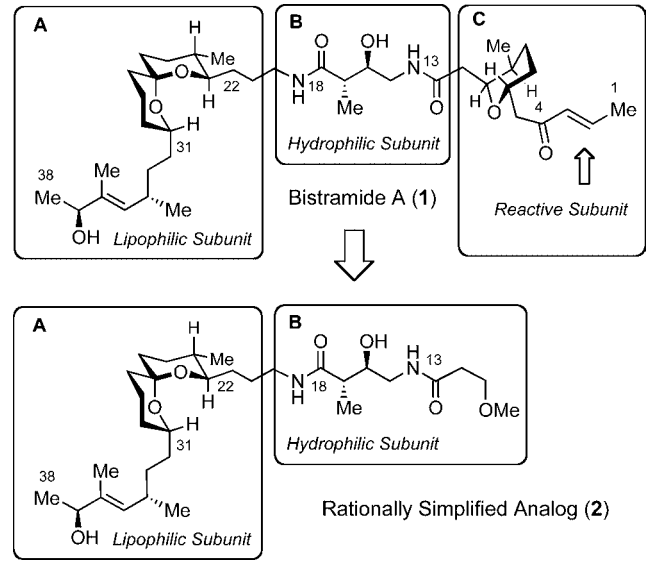

Figure 1. Design of a simplified analog of bistramide A. Liphophilic subunit **A** and hydrophilic subunit **B** are retained to preserve actin-binding and severing activity. Chemically reactive subunit **C** is eliminated to minimize *in vivo* toxicity.

interactions of **2** with actin, which would in turn maximize the potency of this compound.

The assembly process followed our general strategy for rapid polyketide assembly[7,13,14] starting with ring-opening of cyclopropene **4** with alkene **3** in the presence of the Grubbs catalyst **5** (Figure 2A).[15] Removal of the acetal followed by cross-metathesis with alkene **6** delivered dienone **7**. Hydrogenation with concomitant removal of both benzyl and silyl protecting groups and chemoselective installation of the phthalimide moiety, followed by Dess−Martin oxidation, afforded aldehyde **8**; Cr-based olefination and oxazoborolidine reduction afforded phthalimide **9**. The endgame of the synthesis entailed removal of the phthalimide group with methyl amine, PyBOP-promoted coupling with acid **10**,[7] Fmoc-deprotection, and amide coupling using activated ester **12**. This convergent sequence efficiently produced the target compound **2** (11 steps from alkene **3**). It is noteworthy that while the longest linear sequence of the assembly process is comparable to that in our initial synthesis of bistramide A,[7] the total number of steps required for construction of **2** is substantially smaller due to simplification of the subunit **C**.

Isothermal titration calorimetry established the dissociation constant (K_d) value of 9.0 nM for binding of **2** to G-actin, which was comparable to that of the parent natural product **1** (K_d = 6.8 nM)[9] and proved superior to other synthetic bistramide derivatives.[11] The high actin-binding affinity of **2** was attributed to the

[†] Department of Chemistry.
[‡] Department of Molecular Genetics and Cell Biology.
[§] Department of Cellular and Radiation Oncology.

 10.1021/ja101811x

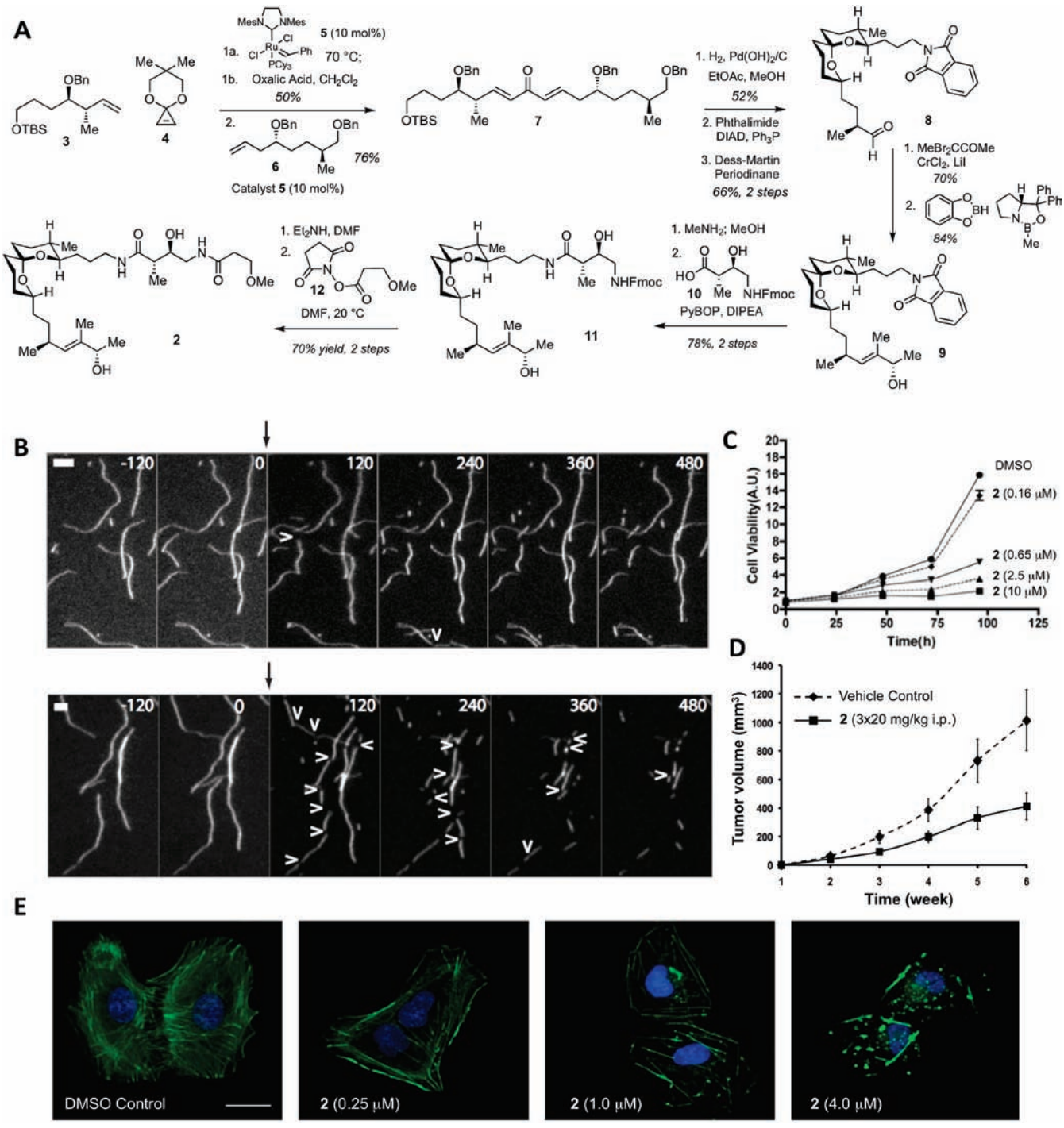

Figure 2. (A) Synthesis of a structurally simplified bistramide analog. This sequence was employed to produce a sufficient amount of **2** (110 mg) for all subsequent studies. (B) Visualization of severing of actin filaments *in vitro* by time-lapse TIRF. Time-lapse micrographs with time in seconds indicated in the upper right. Black arrow at time 0 indicates introduction of one flowcell volume of (top) buffer only or (bottom) buffer containing 1.5 μM of bistramide analog **2**. White arrowheads indicate break points in the filaments. Scale bar $=2.5$ μm. Movies are available as Supporting Information. (C) Time- and dose-dependent growth inhibition of A549 cells by **2**. Cell growth was measured using an ATP-monitoring luciferase-based assay. (D) Growth inhibition of A549 tumors in athymic mice by compound **2**, which was administered i.p. in three doses of 20 mg/kg each on third, fifth, and seventh day after the initial tumor challenge. (E) Depolymerization of F-actin in A549 treated with **2** for 2 h at variable concentrations of the drug shown. Following treatment with **2**, cells were fixed with paraformaldehyde, stained with DAPI (nuclei, blue) and Alexa-fluor 488 phalloidin (actin, green), and imaged using a Leica TCS SP2 AOBS Laser Scanning Confocal microscope. Scale bar $=20$ μm.

van der Waals interactions between several lipophilic amino acid side chains of actin and a fully extended C(31)−C(38) terminus of the spiroketal-bearing subunit **A**. This result further confirmed that pyran-containing fragment **C** did not significantly contribute to the actin-binding affinity of bistramide-based agents.

Encouraged by the initially observed potent G-actin binding affinity of **2**, we next employed time-lapse total internal reflection fluorescence (TIRF) microscopy to examine the effects of this compound on depolymerization of filamentous actin *in vitro*.[16] We initially assembled individual actin filaments by elongating them from a pool of 1.0 μM Mg-ATP-actin monomers supplemented with 0.5 μM Mg-ATP-actin monomers labeled with Oregon green for visualization.[17] We then flowed into the observation chamber either a solution of buffer or a 1.5 μM solution of **2** and imaged

with TIRF microscopy (Figure 2B). As expected, addition of buffer alone did not substantially impact filament depolymerization. On the other hand, treatment of F-actin with **2** resulted in rapid filament disassembly. The mechanism of actin depolymerization by **2** entailed formation of multiple filaments breaks, which created new free barbed ends that rapidly disassemble. This actin-severing mechanism was identical to that displayed by the parent natural product.[11]

We next evaluated the effect of **2** on proliferation of a range of human cancer cell lines grown in culture. This analysis revealed several cell lines that elicited increased sensitivity toward the growth-inhibitory action of this agent, including A549 cells. We next examined the effects of prolonged exposure of **2** on proliferation of this nonsmall lung cancer cell line after 24, 48, 72, and 96 h following initial incubation with this agent (Figure 2C). Cell growth was monitored by measuring the amount of ATP produced using a well-established luciferase-based protocol. This study revealed efficient, dose-dependent growth inhibition. Indeed, the growth of the A549 nonsmall cell lung cancer cell line was inhibited by 70% at 0.65 μM of **2** and by 85% at 2.5 μM of **2**.

We also examined the ability of **2** to depolymerize F-actin in live cells. The actin cytoskeleton can be readily visualized by fluorescent microscopy following Alexa Fluor 488 phalloidin staining. This experiment revealed that **2** depolymerized F-actin in A549 cells in a dose-dependent manner (Figure 2E). Importantly, noticeable actin disassembly was detected even at 250 nM of **2**, which further verified the notable potency of this agent. A similar effect of **2** on F-actin depolymerization was also observed in the DU145 prostate cancer cell line (not shown).

Finally, we examined the ability of **2** to inhibit the growth of A549 cells *in vivo* (Figure 2D). Initially, we established that **2** had no observed toxicity in mice up to a 50 mg/kg single i.p. dose or 3×20 mg/kg i.p. using 3 mice per group with escalating doses starting at 1/10 of those employed for subsequent *in vivo* experiments. Toxicity was assessed by daily weight measurements and mouse behavior compared to noninjected mice. No weight loss (>5%) or behavioral changes were observed. Next, we established tumor xenografts by injecting 1×10^7 A549 cells subcutaneously into two groups of athymic mice. The first group (10 animals) was injected only with the DMSO control. The second group of 12 animals received three i.p. doses of analog **2** (20 mg/kg each) on the third, fifth and seventh day after the initial tumor challenge using the same amount of DSMO as the control group. Tumor growth was monitored over a period of five subsequent weeks every other day. We observed exponential tumor growth in the control mice population, which reached an average size of 731 mm^3 at the end of 5 weeks. Tumor growth was substantially inhibited by analog **2**. The average tumor size for this population was 308 mm^3 after 5 weeks. This result is particularly noteworthy since **2** was administered to animals only during the first week after the initial tumor challenge and no drug was given during the last 5 weeks of the study. These studies demonstrate both a tumor growth delay of 2 weeks and a significant reduction in tumor growth using regression analysis ($p < 0.001$).

Our work demonstrated that a detailed knowledge of biochemistry of the bistramide family of natural products enabled rational design and practical chemical synthesis of a simplified chemical agent **2**, which proved to be highly effective at depolymerizing filamentous actin and inhibiting cancer growth *in vitro* and *in vivo*. Our studies provide a conceptual framework for the design and development of new antiproliferative compounds that target cytoskeletal organization of cancer cells by reversible binding to monomeric actin and effective severing of actin filaments. This work sets the stage for continued comprehensive pharmacological evaluation of this class of actin-targeting agents.[18]

Acknowledgment. Financial support of this work was provided by the American Cancer Society (RSG-04-017-CDD).

Supporting Information Available: Experimental details and movies related to time lapses shown in Figure 2. This information is available free of charge via the Internet at http://pubs.acs.org.

References

(1) Van Troys, M.; Vandekerckhove, J.; Ampe, C. *Protein Rev. 8*; Springer Science and Business Media, LLC: New York, NY, 2008.
(2) (a) Fenteany, G.; Zhu, S. *Curr. Top. Med. Chem.* **2003**, *3*, 593. (b) Spector, I.; Braet, F.; Shochet, N. R.; Bubb, M. R. *Microsc. Res. Tech.* **1999**, *47*, 18. (c) Allingham, J. S.; Klenchin, V. A.; Rayment, I. *Cell. Mol. Life Sci.* **2006**, *63*, 2119.
(3) Gouiffès, D.; Moreau, S.; Helbecque, N.; Bernier, J. L.; Henichart, J. P.; Barbin, Y.; Laurent, D.; Verbist, J. F. *Tetrahedron* **1988**, *44*, 451–459.
(4) Degnan, B. M.; Hawkins, C. J.; Lavin, M. F.; McCaffrey, E. J.; Parry, D. L.; Watters, D. J. *J. Med. Chem.* **1989**, *32*, 1354–1359.
(5) Biard, J. F.; Roussakis, C.; Kornprobst, J. M.; Gouffes-Barbin, D.; Verbist, J. F. *J. Nat. Prod.* **1994**, *57*, 1336–1345.
(6) Murphy, B. T.; Cao, S.; Brodie, P.; Maharavo, J.; Andriamanantoanina, H.; Ravelonandro, P.; Kingston, D. G. I. *J. Nat. Prod.* **2009**, *72*, 1338–1340.
(7) Statsuk, A. V.; Liu, D.; Kozmin, S. A. *J. Am. Chem. Soc.* **2004**, *126*, 9546–9547.
(8) For other synthetic approaches of bistramides, see: (a) Wipf, P.; Uto, Y.; Yoshimura, S. *Chem.—Eur. J.* **2002**, *8*, 1670–1681. (b) Wipf, P.; Hopkins, T. D. *Chem. Commun.* **2005**, 3421–3423. (c) Crimmins, M. T.; DeBaillie, A. C. *J. Am. Chem. Soc.* **2006**, *128*, 4936–4937. (d) Lowe, J. T.; Wrona, I. E.; Panek, J. S. *Org. Lett.* **2007**, *9*, 327–330. (e) Yadav, J. S.; Chetia, L. *Org. Lett.* **2007**, *9*, 4587–4589. (f) Wrona, I. E.; Lowe, J. T.; Turbyville, T. J.; Johnson, T. R.; Beignet, J.; Beutler, J. A.; Panek, J. S. *J. Org. Chem.* **2009**, *74*, 1897–1916.
(9) Statsuk, A. V.; Bai, R.; Baryza, J. L.; Verma, V. A.; Hamel, E.; Wender, P. A.; Kozmin, S. A. *Nat. Chem. Biol.* **2005**, *1*, 383–388.
(10) Rizvi, S. A.; Tereshko, V.; Kossiakoff, A. A.; Kozmin, S. A. *J. Am. Chem. Soc.* **2006**, *128*, 3882–3883.
(11) Rizvi, S. A.; Courson, D. S.; Keller, V. A.; Rock, R. S.; Kozmin, S. A. *Proc. Natl. Acad. Sci. USA.* **2008**, *105*, 4088–4092.
(12) Riou, D.; Roussakis, C.; Biard, J. F.; Verbist, J. F. *Anticancer Res.* **1993**, *13*, 2331–1334.
(13) Marjanovic, J.; Kozmin, S. A. *Angew. Chem., Int. Ed.* **2007**, *46*, 9010–9013.
(14) Matsumoto, K.; Kozmin, S. A. *Adv. Synth. Catal.* **2008**, *350*, 557–560.
(15) Chatterjee, A. K.; Morgan, J. P.; Scholl, M.; Grubbs, R. H. *J. Am. Chem. Soc.* **2000**, *122*, 3783–3784.
(16) (a) Amann, K. J.; Pollard, T. D. *Proc. Natl. Acad. Sci. U.S.A.* **2001**, *98*, 15009–15013. (b) Kovar, D. R.; Pollard, T. D. *Proc. Natl. Acad. Sci. U.S.A.* **2004**, *101*, 14725–14730. (c) Kovar, D. R.; Harris, E. S.; Mahaffy, R.; Higgs, H. N.; Pollard, T. D. *Cell* **2006**, *124*, 423–435.
(17) Neidt, E. M.; Skau, C. T.; Kovar, D. R. *J. Biol. Chem.* **2008**, *283*, 23872–23883.
(18) Compound **2** has been selected for preclinical pharmacological study by the National Cancer Institute's (NCI's) Rapid Access to Interventional Development (RAID) program; NSC Number: D751592-H.

JA101811X